



Variation of mean sea surface temperature and modulation of El Niño–Southern Oscillation variance during the past 150 years

Yue Fang,¹ John C. H. Chiang,¹ and Ping Chang²

Received 24 February 2008; revised 20 April 2008; accepted 8 May 2008; published 31 July 2008.

[1] Evidence is presented that the dominant non-trend mode of interdecadal global SST variations is linked to significant modulation of ENSO variance during the past 150 years. The mode resembles the interhemispheric SST pattern linked to Sahel rainfall changes, with colder northern hemisphere conditions co-incident with higher ENSO variance. Simulations of an intermediate coupled global climate model demonstrate that this global SST pattern can drive the interdecadal changes to ENSO variance. The influence on the ENSO dynamics comes primarily from the portion of the SST change local to the tropical Pacific, which is warm over the entire equatorial Pacific particularly in the southeast during times of stronger ENSO activity. We speculate that the warming equatorial SST causes ENSO events occur earlier and thus have longer time to develop, as well as enhancing the vertical temperature gradient and thus increasing the effectiveness of oceanic entrainment. **Citation:** Fang, Y., J. C. H. Chiang, and P. Chang (2008), Variation of mean sea surface temperature and modulation of El Niño–Southern Oscillation variance during the past 150 years, *Geophys. Res. Lett.*, 35, L14709, doi:10.1029/2008GL033761.

1. Introduction

[2] The El Niño–Southern Oscillation (ENSO) exhibits variations on decadal to multidecadal timescales in its properties including amplitude, period, phase locking, and propagation. There is no consensus about what mechanism is responsible for the interdecadal variation of ENSO. Some studies [e.g., *Flugel et al.*, 2004; *Kirtman et al.*, 2005] show that the stochastic forcing and chaotic dynamics may cause change in some ENSO properties, while other studies [e.g., *Wang*, 1995; *Fedorov and Philander*, 2001; *Dong et al.*, 2006] propose that the modulation of ENSO is caused by the change in mean state. In addition, some recent studies [e.g., *Rodgers et al.*, 2004; *Schopf and Burgman*, 2006] argue that the change in mean state is perhaps just a residual effect due to the asymmetry between El Niño and La Niña events.

[3] In this paper, we demonstrate that a dominant mode of interdecadal variation in SST is causally linked to the changes in ENSO variance over the 20th century. This mode has been previously identified and implicated in interdecadal Sahel rainfall changes. We show by means of an intermediate coupled model designed for ENSO studies that

the SST pattern associated with this mode can drive the ENSO variance change, and that furthermore the ENSO changes appear to result from the changes to the tropical Pacific mean state.

2. ENSO Variance and Mean SST

[4] We first show the multidecadal changes to ENSO variance from a running 21-year window based on the time series of Niño-3 SST index (defined as mean SST anomaly in 5°S–5°N, 150°–90°W) derived from HadISST [*Rayner et al.*, 2003] from 1870–2004. Prior to the calculation of Niño-3 index, a 7-year running mean is removed from the observed monthly SST anomalies in order to remove the decadal and longer SST variability. The dashed line in Figure 1b is the linearly detrended time series of ENSO variance, which shows a minimum in 1950s and increases rapidly thereafter.

[5] To extract possible global-scale multidecadal variations linked to ENSO variance, an EOF analysis is done in a global domain from 40°S–60°N using observed SST anomalies that has first been low-passed by a 21-year running mean. The first three EOFs explain 68%, 15%, and 7% of total low-frequency variance, respectively, and they are well separated from each other. The first EOF is the global warming trend (figure not shown); the second EOF is shown in Figure 1 and the SST pattern appears robust: repeating the same analysis using *Kaplan et al.* [1998] SST anomalies yields similar results; we've also tried repeating the EOF analysis on detrended SST, and the first mode extracted is similar to the EOF shown in Figure 1. Similar SST anomaly fields have also been derived in previous studies using different methods and datasets [*Zhang et al.*, 1997]. This gives us confidence that we have extracted is a physically-meaningful spatial pattern of low-frequency SST variability from existing observational data.

[6] The PC time series closely matches the change of ENSO variance on multidecadal timescales (Figure 1b), correlated at 0.7. Since the SST anomaly in Figure 1a exhibits a complex global structure, and it is quite different from the residual SST structure due to the asymmetry of SST anomalies associated with El Niño and La Niña events [*Rodgers et al.*, 2004], we can confidently rule out the possibility that the SST variability represented by the second EOF is a result of ENSO nonlinearity. Therefore, we hypothesize that the modulation of ENSO variance is caused by the change of mean SST shown in Figure 1.

3. Model and Experiments

[7] To explore the mechanisms of linkage between mean SST and ENSO variance, we employed an intermediate

¹Department of Geography and Center for Atmospheric Sciences, University of California, Berkeley, California, USA.

²Department of Oceanography, Texas A&M University, College Station, Texas, USA.

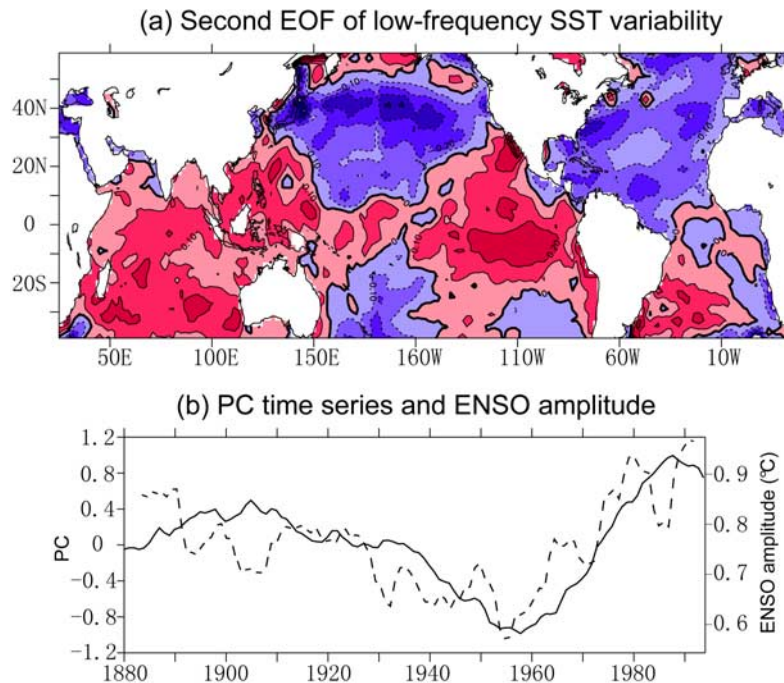


Figure 1. (a) Second EOF of low-frequency (21-year low-pass) SST variability and (b) corresponding PC time series (solid line, normalized to 1) and standard deviation of Niño-3 SST index (dashed line) derived from HadISST [Rayner *et al.*, 2003]. The contour interval is 0.1°C . Red areas denotes warm SST anomalies. The standard deviation is calculated in a running 21-year window based on 7-year high-pass monthly SST anomalies, and the linear trend of the curve is removed.

coupled model. The atmospheric component is the Community Climate Model version 3 (CCM3) in standard configuration (T42 resolution, 18 hybrid levels) [Kiehl *et al.*, 1998]. The oceanic component is a derivative of the Zebiak and Cane [1987] 1.5-layer reduced-gravity ocean model with a resolution of 2×1 degree in longitude-latitude. Previous version of this coupled model has successfully simulated tropical climate variability in many studies [Fang, 2005; Chang *et al.*, 2006, 2007]. The major improvement of present model is that the model domain is now expanded globally to $80^{\circ}\text{S}/\text{N}$, and the full surface fluxes are now passed between the atmosphere and ocean, as opposed to anomalous flux coupling used in the previous versions. More details of our model and its simulation characteristics are in the supplementary material.¹

[8] Two experiments (Global Ocean experiment and Tropical Pacific experiment) are carried out to investigate the influence of mean SST on ENSO variance, and each experiment has two runs, which correspond to the warm period (1980–2000) and cold period (1950–1970) in the equatorial Pacific as shown in Figure 1b. In the Global Ocean experiment, we use the long-term mean climatology from 1870–2004 plus or minus the SST anomaly shown in Figure 1a as the SST climatology during warm period and cold period, respectively. The different climatologies are imposed on the model through the flux correction applied to the model; an iterative procedure was developed to obtain the flux correction necessary to produce the appropriate climatology. A projection of observational SST anomalies onto the second EOF (Figure 1a) does not show any

seasonality, so applying the SST anomaly equally throughout the year is valid. The Tropical Pacific experiment is same as the Global Ocean experiment except that the anomaly shown in Figure 1a is only applied to the tropical Pacific ($25^{\circ}\text{S}\sim 25^{\circ}\text{N}$). Comparison between the two experiments can tell us how much influence comes from SST forcing of extratropical Pacific and the other oceans.

4. Results

[9] Figures 2a and 2b show the monthly Niño-3 SST index simulated by the Global Ocean experiment. The standard deviations of Niño-3 SST index of the cold period run and warm period run are 0.58°C and 0.76°C , respectively. The magnitude of the change in ENSO amplitude simulated by model (31% increase) is in good agreement with the observation ($\sim 38\%$ increase from the period 1950–1970 to period 1980–2000). In addition to the larger amplitude, the ENSO associated with warm period run also exhibits a longer oscillation period (3.9 years compared to 3.3 years in cold period run) (Figure 2c), qualitatively consistent with the observed ENSO period change during the two periods [An and Wang, 2000]. Figure 2d presents the composites of SST evolution in Niño-3 region during modeled El Niño events. Both the amplitude and period changes are shown clearly.

[10] How does the change of mean SST cause substantial change in ENSO amplitude and period? To answer this question, we examine the difference in surface wind stress and precipitation rate between the cold period run and the warm period run (the latter minus the former). In Figure 3a, there is a strong wind anomaly in the deep tropic of Pacific, expanding from Date Line to the west coast of South

¹Auxiliary materials are available in the HTML. doi:10.1029/2008GL033761.

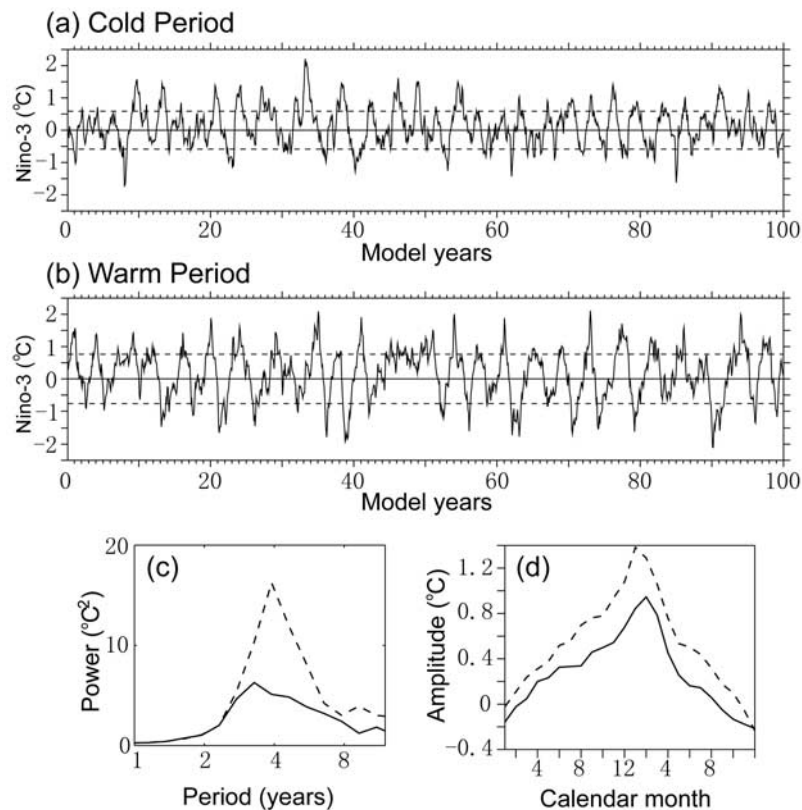


Figure 2. Niño-3 SST indices of Global Ocean (a) cold period run, (b) warm period run, and (c) corresponding power spectrums. (d) Composite of SST evolution in Niño-3 region during modeled El Niño events based on 100-year simulations. Dashed lines in Figures 2a and 2b are one standard deviation limits. Solid (dashed) line in Figures 2c and 2d is for cold (warm) period run.

America. This wind anomaly is a direct response to the warming of underlying SST when the mean state shift from cold period to warm period. Similar anomalous wind field (figures not shown) can also be found in ECMWF ERA-40 [Uppala *et al.*, 2005] and NCEP/NCAR reanalysis [Kalnay *et al.*, 1996] dataset by calculating the difference between periods 1950–1970 and 1980–2000.

[11] The wind anomaly is associated with the equatorward shift of the intertropical convergence zone (ITCZ), as shown in the precipitation pattern (Figure 3b). In the central and eastern Pacific, the precipitation to the south of equator is enhanced while that to the north of equator is suppressed. Previous studies [e.g., Philander, 1985; Zebiak and Cane, 1987] found that the boreal spring is the most favorable time for a warm anomaly in the eastern equatorial Pacific to cause anomalous local atmospheric heating because during this season the ITCZ is at its southernmost extreme and SST is at a seasonal maximum. The enhanced southward shift of ITCZ during the warm period makes this favorable season come earlier, causing ENSO events start earlier and have longer time to develop, thus stronger ENSO amplitude (Figure 2d) even if the atmosphere-ocean coupling strength keeps unchanged. The shift of ITCZ may also postpone the unfavorable season of ENSO, causing ENSO events end later. This may explain why the ENSO was stronger and its period was longer since 1980s.

[12] The change of mean SST also changes the vertical stratification of upper ocean. Contrasting the simulated mean depth of thermocline between the cold period and

warm period runs (the latter minus the former; figure not shown) shows that the change in thermocline is mainly located at latitudes higher than 10°S/N in the western Pacific, while there is little change in the deep tropics of the Pacific. In general, the mean thermocline along the equator during warm period is shallower than that during cold period (dashed line in Figure 4). The shoaling in thermocline is qualitatively consistent with what Levitus *et al.* [1994] data and SODA data [Carton *et al.*, 2000] suggest (Figure 4). Since we usually choose 20°C isotherm as thermocline depth, a ~ 2 m shoaling in thermocline combined with a $\sim 0.35^{\circ}\text{C}$ increase in SST from cold period to warm period can induce $\sim 10\%$ increase in thermocline temperature gradient in the Niño-3 region. Therefore, during warm period, the same perturbations in thermocline depth produce a larger subsurface temperature anomaly and thus translate into larger SST variations. The model results do show an increase in the regression coefficient (from 0.034°C/m in the cold period run to 0.038°C/m in the warm period run) of SST anomaly against thermocline perturbation in the Niño-3 region when SST lags thermocline by 3 months. Therefore, the enhanced temperature gradient in thermocline may also play an important role in enhancing ENSO amplitude after 1980s.

[13] How much influence on ENSO does it come from SST in oceans other than tropical Pacific? A similar analysis is conducted on the output of Tropical Pacific experiment, and the results (Figure S5¹ in supplementary material) show that the change in ENSO is basically same as what is found

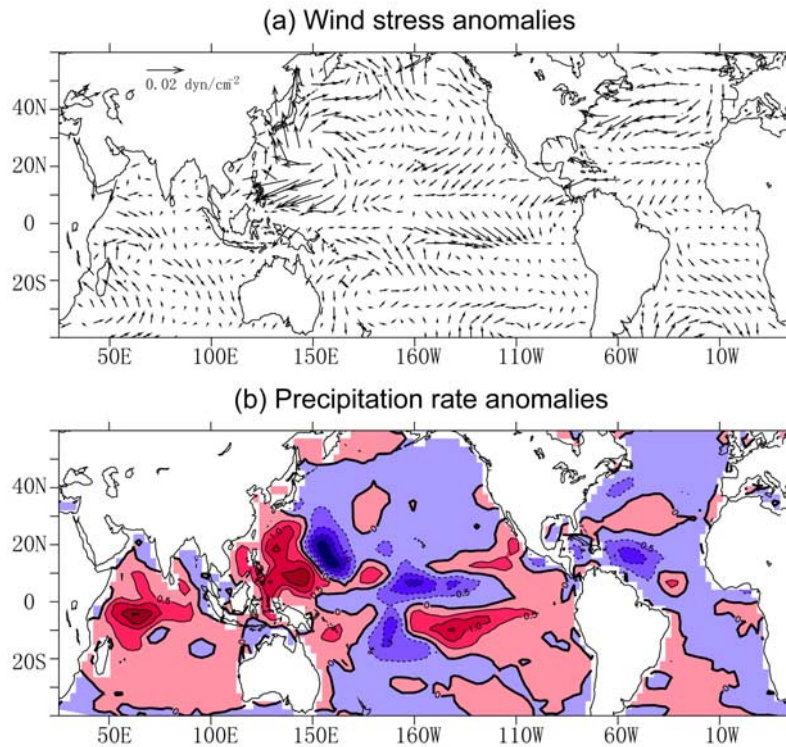


Figure 3. Difference in climatological annual mean (a) surface wind stress and (b) precipitation rate between Global Ocean cold period and warm period runs (the latter minus the former). Contour interval is 0.5mm/day. Red areas denote increase in precipitation rate.

in Global Ocean runs (Tropical Pacific experiment shows 30% increase in variance and ~ 7 months increase in period from cold period to warm period). This is not surprising because similar change in surface wind stress, precipitation rate, and thermocline depth are also found in the Tropical Pacific simulations. These results suggest that the change in mean SST outside the tropical Pacific shown in Figure 1a has little direct impact on ENSO variance and period.

5. Summary and Discussion

[14] Understanding the mechanisms of the change of ENSO properties is important for the prediction of ENSO variability and its potential impact on the future climate. Using EOF analysis and observational data, the dominant non-trend mode of interdecadal global SST variations is shown to be linked to the modulation of ENSO variance and period during the past 150 years. By imposing this global SST pattern on an intermediate coupled model, we were able to simulate the changes to the ENSO variance and period consistent with observations. The changes to the ENSO are thought to be associated with a shift in the ITCZ induced by the global SST pattern: a southward shift prolongs the favorable season of ENSO growth, causing larger ENSO amplitude and longer period. The warming in SST along with the shoaling of thermocline also enhances the temperature gradient in thermocline and thus induces stronger subsurface response to the surface wind forcing.

[15] If our result turns out to be true, then determining the causes of the interdecadal global SST variation in Figure 1a would be of tremendous interest. While our results suggest that it is the SST variations local to the tropical Pacific that

are responsible for the ENSO variance changes, the fact that they are part of a global mode of SST variation suggests that the origins of these changes may not be local to the tropical Pacific. This interpretation is supported by the fact that Sahel rainfall is also associated with similar global SST pattern [e.g., Folland *et al.*, 1986]. Previous studies have suggested Atlantic thermohaline variations [e.g., Zhang and

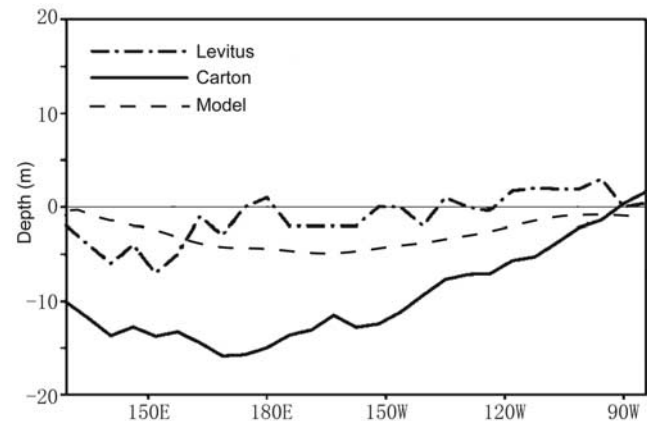


Figure 4. Difference (dashed line) in mean depth of 20 °C isotherm between Global Ocean cold period and warm period runs (the latter minus the former). The solid line and dash-dotted line from Wang and An [2002] are the difference between 1961–1975 and 1981–1995 periods derived from Levitus *et al.* [1994] data and SODA data [Carton *et al.*, 2000], respectively.

Delworth, 2006] or anthropogenic aerosol forcing [e.g., Biasutti and Giannini, 2006; Rotstayn and Lohmann, 2002] to be linked to Sahel rainfall variations; such sources of northern hemisphere cooling can be propagated to the tropical marine climate through atmospheric teleconnections [e.g., Broccoli et al., 2006; Chiang and Bitz, 2005].

[16] Two previous studies have explored influence of mean state on ENSO variability by forcing models using observed data, but a full satisfactory picture of the mechanism is still to emerge. Wang and An [2002] argue for decadal changes of background equatorial winds and associated upwelling in the Pacific to change ENSO. However, there is uncertainty in how exactly the surface winds in the eastern equatorial Pacific changed between their earlier (1961–1975) and later (1981–1995) periods (1961–1975 and 1981–1995); we found that the wind changes derived from ECMWF ERA-40 and NCEP/NCAR reanalysis to be quite different from the FSU winds they used [Wang and An, 2002, Figure 2a]. Modeling work by Dong et al. [2006] found that warming of the North Atlantic and cooling of the south Atlantic, associated with the Atlantic Multidecadal Oscillation (AMO), can deepen the mean thermocline and reduce vertical stratification, thus leads to a reduction in ENSO variability. The AMO index and ENSO magnitude appear to vary in sync before 1980s. However, after 1980s when ENSO is strongest, as also noted by Dong et al. [2006, Figure 1b], increasing ENSO variance is accompanied by the warming of the North Atlantic.

[17] **Acknowledgments.** This work is supported by grants from the National Science Foundation ATM-0438201 and the Comer Science and Education Foundation.

References

- An, S.-L., and B. Wang (2000), Interdecadal change of the structure of the ENSO mode and its impact on the ENSO frequency, *J. Clim.*, *13*, 2044–2055.
- Biasutti, M., and A. Giannini (2006), Robust Sahel drying in response to late 20th century forcings, *Geophys. Res. Lett.*, *33*, L11706, doi:10.1029/2006GL026067.
- Broccoli, A. J., K. A. Dahl, and R. J. Stouffer (2006), Response of the ITCZ to Northern Hemisphere cooling, *Geophys. Res. Lett.*, *33*, L01702, doi:10.1029/2005GL024546.
- Carton, J. A., G. Chepurin, X. Cao, and B. Giese (2000), A simple ocean data assimilation analysis of the global upper ocean 1950–95. Part I: Methodology, *J. Phys. Oceanogr.*, *30*, 294–309.
- Chang, P., Y. Fang, R. Saravanan, L. Ji, and H. Seidel (2006), The cause of the fragile relationship between the Pacific El Niño and the Atlantic Niño, *Nature*, *443*, 324–328, doi:10.1038/nature05053.
- Chang, P., L. Zhang, R. Saravanan, D. J. Vimont, J. C. H. Chiang, L. Ji, H. Seidel, and M. K. Tippett (2007), Pacific meridional mode and El Niño–Southern Oscillation, *Geophys. Res. Lett.*, *34*, L16608, doi:10.1029/2007GL030302.
- Chiang, J. C. H., and C. M. Bitz (2005), Influence of high latitude ice cover on the marine Intertropical Convergence Zone, *Clim. Dyn.*, *25*, 477–496.
- Dong, B., R. T. Sutton, and A. A. Scaife (2006), Multidecadal modulation of El Niño–Southern Oscillation (ENSO) variance by Atlantic Ocean sea surface temperatures, *Geophys. Res. Lett.*, *33*, L08705, doi:10.1029/2006GL025766.
- Fang, Y. (2005), A coupled model study of the remote influence of ENSO on tropical Atlantic SST variability, Ph.D. dissertation, Tex. A&M Univ., College Station.
- Fedorov, A. V., and S. G. Philander (2001), A stability analysis of tropical ocean–atmosphere interactions: Bridging measurements and theory for El Niño, *J. Clim.*, *14*, 3086–3101.
- Folland, C. K., T. N. Palmer, and D. E. Parker (1986), Sahel rainfall and worldwide sea temperatures, 1901–85, *Nature*, *320*, 602–607.
- Flugel, M., P. Chang, and C. Penland (2004), The role of stochastic forcing in modulating ENSO predictability, *J. Clim.*, *17*, 3125–3140.
- Kalnay, E., et al. (1996), The NCEP/NCAR 40-year reanalysis project, *Bull. Am. Meteorol. Soc.*, *77*, 437–470.
- Kaplan, A., M. A. Cane, Y. Kushnir, A. C. Clement, M. B. Blumenthal, and B. Rajagopalan (1998), Analyses of global sea surface temperature 1856–1991, *J. Geophys. Res.*, *103*, 18,567–18,589.
- Kiehl, J. T., J. J. Hack, G. B. Bonan, B. A. Boville, D. L. Williamson, and P. J. Rasch (1998), The National Center for Atmospheric Research Community Climate Model: CCM3, *J. Clim.*, *11*, 1131–1149.
- Kirtman, B. P., K. Pegion, and S. Kinter (2005), Internal atmospheric dynamics and tropical Indo-Pacific climate variability, *J. Atmos. Sci.*, *62*, 2220–2233.
- Levitus, S., T. P. Boyer, and J. Antonov (1994), *World Ocean Atlas 1994*, vol. 5, *Interannual Variability of Upper Ocean Thermal Structure*, NOAA Atlas NESDIS, vol. 5, 176 pp., NOAA, Silver Spring, Md.
- Philander, S. G. H. (1985), El Niño and La Niña, *J. Atmos. Sci.*, *42*, 2652–2662.
- Rayner, N. A., D. E. Parker, E. B. Horton, C. K. Folland, L. V. Alexander, D. P. Rowell, E. C. Kent, and A. Kaplan (2003), Global analyses of sea surface temperature, sea ice, and night marine air temperature since the late nineteenth century, *J. Geophys. Res.*, *108*(D14), 4407, doi:10.1029/2002JD002670.
- Rodgers, K. B., P. Friederichs, and M. Latif (2004), Tropical Pacific decadal variability and its relation to decadal modulations of ENSO, *J. Clim.*, *17*, 3761–3774.
- Rotstayn, L. D., and U. Lohmann (2002), Tropical rainfall trends and the indirect aerosol effect, *J. Clim.*, *15*, 2103–2116.
- Schopf, P. S., and R. J. Burgman (2006), A simple mechanism for ENSO residuals and asymmetry, *J. Clim.*, *19*, 3167–3179.
- Uppala, S. M., et al. (2005), The ERA-40 re-analysis, *Q.J.R. Meteorol. Soc.*, *131*, 2961–3012.
- Wang, B. (1995), Interdecadal changes in El Niño onset in the last four decades, *J. Clim.*, *8*, 267–285.
- Zebiak, S. E., and M. A. Cane (1987), A model El Niño–Southern Oscillation, *Mon. Weather Rev.*, *115*, 2262–2278.
- Zhang, R., and T. L. Delworth (2006), Impact of Atlantic multidecadal oscillations on India/Sahel rainfall and Atlantic hurricanes, *Geophys. Res. Lett.*, *33*, L17712, doi:10.1029/2006GL026267.
- Zhang, Y., J. M. Wallace, and D. Battisti (1997), ENSO-like interdecadal variability: 1900–93, *J. Clim.*, *10*, 1004–1020.

P. Chang, Department of Oceanography, Texas A&M University, College Station, TX 77843, USA.

J. C. H. Chiang and Y. Fang, Department of Geography, University of California, Berkeley, CA 94720, USA. (yfang@atmos.berkeley.edu)